

Revised Primordial Helium Abundance Based on New Atomic Data

Manuel Peimbert

*Instituto de Astronomía, Universidad Nacional Autónoma de México, Apdo. Postal 70-264,
México 04510 D.F., Mexico*

peimbert@astroscu.unam.mx

Valentina Luridiana

*Instituto de Astrofísica de Andalucía (CSIC), Camino Bajo de Huétor 50, 18008 Granada,
Spain*

vale@iaa.es

and

Antonio Peimbert

*Instituto de Astronomía, Universidad Nacional Autónoma de México, Apdo. Postal 70-264,
México 04510 D.F., Mexico*

antonio@astroscu.unam.mx

ABSTRACT

We have derived a primordial helium abundance of $Y_p = 0.2477 \pm 0.0029$, based on new atomic physics computations of the recombination coefficients of He I and of the collisional excitation of the H I Balmer lines together with observations and photoionization models of metal-poor extragalactic H II regions. The new atomic data increase our previous determination of Y_p by 0.0086, a very significant amount. By combining our Y_p result with the predictions made by the standard Big Bang nucleosynthesis model, we find a baryon-to-photon ratio, η , in excellent agreement both with the η value derived by the primordial deuterium abundance value observed in damped Lyman- α systems and with the one obtained from the WMAP observations.

Subject headings: early universe — galaxies: abundances — galaxies: individual (SBS 0335–052, I Zw 18, Haro 29) — galaxies: ISM — H II regions — ISM: abundances

1. Introduction

This is the third paper of a series on the determination of the primordial helium abundance by unit mass, Y_p . In Paper I (Peimbert et al. 2002) we studied the effect of temperature variations on the determination of Y_p , and in Paper II (Luridiana et al. 2003) we studied the effect of collisional excitation of the Balmer lines in the determination of Y_p .

The determination of Y_p is important for the study of cosmology and the chemical evolution of galaxies. In particular, Y_p can be used to test the standard Big Bang nucleosynthesis (SBBN) scenario by setting strong constraints on: a) the number of neutrino families, N_ν ; b) the variation of the neutron lifetime and of the neutron-proton mass difference, these constraints can be translated into constraints on the time variation of the Yukawa couplings and the fine structure constant; c) the variation of the constant of gravity, G ; d) the presence of vacuum energy during BBN; and e) the presence of decaying particles during BBN, which could have affected the production of the light elements (e.g. Cyburt et al. 2005; Coc et al. 2006, and references therein). The accuracy in Y_p needed to reach these goals extends to the third decimal place (e.g. Peimbert et al. 2003; Luridiana 2003; Steigman 2006a). Y_p determinations are affected by at least thirteen sources of error (see Section 3 and the review by Peimbert et al. 2003). In Paper II we obtained a determination of Y_p in which most of these sources of error were taken into account. In this paper we improve our previous Y_p determination, considering new atomic data and improved stellar population synthesis models, which are likely to further reduce the error affecting our computation. Specifically, four of the main sources of error are reduced by means of the use of: a) the recent He I recombination coefficients by Porter et al. (2005, 2007), b) the H I collisional excitation coefficients by Anderson et al. (2000, 2002), and c) the correction for underlying absorption for lines redward of 5000 Å, based on the population synthesis models by González Delgado et al. (2005) and the observations by Leone & Lanzafame (1998).

Y_p is determined by means of an extrapolation to $Z = 0$ of the Y values of a sample of objects. Here, the usual normalization $X + Y + Z = 1$ is used, where X , Y , and Z are the abundances per unit mass of hydrogen, helium, and the rest of the elements respectively. The extrapolation is traditionally done in the Y, Z space by assuming a $\Delta Y/\Delta Z$ slope (Peimbert & Torres-Peimbert 1974). More recently it has become common to use $\Delta Y/\Delta O$, where O is the oxygen abundance per unit mass, since the O value is easier to determine.

In Section 2 we discuss the collisional excitation of the Balmer lines and apply the corresponding correction to our H II regions sample. In Section 3 we correct the observed line intensities by extinction and underlying absorption, also in this section we determine the Y values for each of the objects of the sample, and combining them with a $\Delta Y/\Delta O$ relationship we derive the new Y_p value. In this section we present the error budget of

our determination and a discussion is made where we distinguish between systematic and statistical effects. In Section 4 we compare our determination with those by other authors. In Section 5 we discuss the cosmological implications of our new Y_p value, and in Sections 6 and 7 we present the discussion and our conclusions. A preliminary account of some of the results included in this paper was presented elsewhere (Peimbert et al. 2007).

2. Collisional enhancement of hydrogen Balmer lines

In high-temperature H II regions, the hydrogen Balmer lines can be excited by collisions of neutral atoms with free electrons. This effect is generally small, usually contributing less than a few percent of the intensity of $H\alpha$ and $H\beta$ or less, which for most applications can be neglected. However, collisional enhancement must be taken into account in the determination of Y_p for at least two reasons. First, for this task the helium abundance by unit mass, Y , in individual H II regions must be known with the highest attainable precision. Second, the objects where collisions are more important are those with the highest T_e and, hence, the lowest metallicities; consequently, they bear a major weight in the extrapolation to $Z = 0$ of the relation between Y and Z .

In Paper II we used photoionization models calculated with the photoionization code Cloudy to estimate the collisional contribution to the Balmer lines in five low-metallicity objects. For three objects (Haro 29, I Zw 18, and SBS 0335-052) we computed tailored models using version 94.00 of Cloudy, last described by Ferland et al. (1998); for the remaining two objects (NGC 2363 and NGC 346) the models were retrieved from previously published works (Luridiana et al. 1999; Relaño et al. 2002, respectively), and the collisional rate in them was estimated from the difference between the total and the case B $H\beta$ emission predicted by the models. In the present work, we present improved estimates, which differ from the previous ones in several aspects: a) The models for NGC 2363 and NGC 346 have been recalculated based on the input parameters described in the original papers, so that the collisional contribution could be explicitly computed rather than simply estimated; b) the collisional rates have been updated; c) the radiative cascade following collisional excitation is now computed self-consistently, and d) the model fitting follows a different philosophy with respect to Paper II. Points b), c) and d) will be explained in detail in the following sections. A further difference with respect to Paper II is that, while the collisional luminosities of Paper II models had been computed simultaneously with the models themselves by modifying a Cloudy’s routine, those of the present paper have been computed by an external program, to which Cloudy’s output (i.e., the ionization and temperature structures) is fed. The difference between the two procedures is, of course, irrelevant from the point of view of results, except

for the change in the collisional atomic data used in either case, which will be discussed in Section 2.1.

2.1. Updated collisional rates

In previous works, it has been estimated that $I(\text{H}\beta)_{\text{col}}/I(\text{H}\alpha)_{\text{col}}$ is about 1/10 (Davidson & Kinman 1985; Stasińska & Izotov 2001; Luridiana et al. 2003), and it has been predicted that this differential enhancement would increase the observed Balmer decrement, mimicking a larger interstellar reddening. The amount of extra reddening due to this mechanism is expressed by the collisional reddening coefficient $C(\text{H}\beta)^{\text{col}}$:

$$\begin{aligned} C(\text{H}\beta)^{\text{col}} &= \frac{\text{Log}(I(\text{H}\alpha)^{\text{tot}}/I(\text{H}\beta)^{\text{tot}}) - \text{Log}(I(\text{H}\alpha)^{\text{rec}}/I(\text{H}\beta)^{\text{rec}})}{-f(\text{H}\alpha)} = \\ &= \frac{\text{Log}((1 - I(\text{H}\beta)^{\text{col}}/I(\text{H}\beta)^{\text{tot}})/(1 - I(\text{H}\alpha)^{\text{col}}/I(\text{H}\alpha)^{\text{tot}}))}{-f(\text{H}\alpha)} = \\ &\equiv \frac{\text{Log}((1 - x_\beta)/(1 - x_\alpha))}{-f(\text{H}\alpha)}, \end{aligned} \quad (1)$$

where $I(\lambda)_{\text{rec}}/I(\lambda)_{\text{tot}}$ and $x_\lambda \equiv I(\lambda)_{\text{col}}/I(\lambda)_{\text{tot}}$ are the relative contributions of recombinations and collisions, respectively, to the total emitted intensity in λ , and $f(\text{H}\alpha)$ is the reddening correction at $\text{H}\alpha$. Collisional and interstellar reddening add together to yield the observed reddening:

$$C(\text{H}\beta)^{\text{obs}} = C(\text{H}\beta)^{\text{dust}} + C(\text{H}\beta)^{\text{col}}, \quad (2)$$

(see Paper II), so that a good estimate of $C(\text{H}\beta)^{\text{col}}$ is needed to properly derive $C(\text{H}\beta)^{\text{dust}}$ from the observed reddening.

In the present work we have used updated collisional coefficients (Anderson et al. 2000, 2002) to revise our previous estimates of x_α and x_β and the derived value of $C(\text{H}\beta)^{\text{col}}$. Two major features of the new data deserve to be noted here in comparison to those used in Paper II (Callaway 1994; Vriens & Smeets 1980):

1. All the collisional coefficients $\Omega(1, n)$, to which collisional rates are directly proportional, are larger than the corresponding values by Callaway (1994) and Vriens & Smeets (1980) in the temperature range of interest.

⁰The reference to Anderson et al. (2000) and Anderson et al. (2002) contained in Paper II was erroneous, as the models had been computed with an earlier version of Cloudy.

2. The increase of $\Omega(1, 4)$ is larger than that of $\Omega(1, 3)$ by a factor of 2.5 approximately.

Point 1 above implies larger collisional contributions to all Balmer lines than previously estimated. Point 2 implies that $I(\text{H}\beta)_{\text{col}}/I(\text{H}\alpha)_{\text{col}}$ also increases by (roughly) the same factor of 2.5 as $\Omega(1, 4)/\Omega(1, 3)$. This is because, although collisional excitations to any level with $n \geq 3$ might eventually produce an $\text{H}\alpha$ photon, excitations to $n = 3$ largely dominate and are responsible for more than 80% of the collisional $\text{H}\alpha$ emission in our objects; analogously, excitations to $n = 4$ dominate the collisional $\text{H}\beta$ emission, yielding more than 90% of it. Therefore, the predicted $I(\text{H}\beta)_{\text{col}}/I(\text{H}\alpha)_{\text{col}}$ closely follows the $\Omega(1, 4)/\Omega(1, 3)$ ratio: with the data by Anderson et al. (2000, 2002) it is now predicted to be larger than 1/4 at $T_e = 20000$ K and approaching 1/3 at larger temperatures, making it almost indistinguishable from the normal Balmer decrement produced by recombinations. As a result, with the updated collisional coefficients $C(\text{H}\beta)^{\text{col}}$ is predicted to be much smaller than previously estimated, and a larger fraction of the observed reddening can be attributed to dust interstellar reddening.

2.2. Improved radiative cascade

In addition to using the new collisional coefficients, we have now improved our scheme for the calculation of the radiative cascade following a collisional excitation. The collisional data used in Paper II were available only as level-averaged coefficients $\Omega(n)$, whereas the new coefficients are available as $\Omega(n, l)$. Therefore, an ad-hoc assumption had to be made in Paper II regarding how electrons excited by collisions distribute themselves among the sublevels (n, l) of a given level n ; this assumption, in turn, determined the radiative spectrum following an upward collision. In the present work, in contrast, knowledge of the $\Omega(n, l)$ makes it straightforward to calculate the radiative cascade following upward collisions, and no assumptions are required (for low values of n , l -mixing is completely negligible at the densities of our objects, $N_e \lesssim 1000 \text{ cm}^{-3}$).

2.3. Model fitting

Because the collisional enhancement of Balmer lines depends on the interplay between the abundance of H^0 and the temperature structure of the region, good estimates can only be given with tailored photoionization models that simultaneously constrain the temperature and the ionization structure. In Paper II, we computed several tailored photoionization models for each of the three high- T_e H II regions SBS 0335-052, I Zw 18 and Haro 29, and estimated the collisional enhancement of $\text{H}\alpha$ and $\text{H}\beta$ by selecting those models that

properly fit the observed [O III] temperature, without bothering about the fitting of T [O II]. The rationale of that choice was that, because of the Boltzmann factor in the expression for the collisional rate, the temperature dependence of collisional rates is very strong: as a consequence, we thought that an accurate estimate could only be granted by a good fit of the hottest region of the nebula, which in this range of metallicities is the inner one and is characterized by the [O III] temperature.

However, further calculations have shown that, in most cases, the dominant contribution to the collisional excitation of hydrogen comes from the outer zones. This happens because the outward increase in the fraction of neutral hydrogen outweighs the decrease in temperature, exceptions to this behavior will be mentioned in Section 6 and extensively discussed in a forthcoming paper (Luridiana, in preparation). Since the outer zones are best characterized by the [O II] temperature, the collisional contribution to Balmer lines is now computed based on models that correctly fit the [O II] rather than the [O III] temperature. An example of this behavior is given in Fig. 1, which shows, for one of our model nebulae, the relative contribution of each layer to the emission in the [O II] and [O III] lines and in $H\beta_{\text{col}}$. The three panels correspond to different integrations, simulating a beam (i.e., a point-like slit), a narrow slit, and a slit covering the whole object respectively; depending on how the nebula is sampled by the aperture, different layers contribute differently to the overall emission. In all cases, we can see that the collisional $H\beta$ emission closely follows the emission of the [O II] lines: in other words, $H\beta_{\text{col}}$ preferentially forms in the [O II] rather than in the [O III] zone. The effect is more pronounced in the case of a beam, which is a good approximation for the data of four of our five objects, but is still seen even in the case in which the whole nebula is sampled.

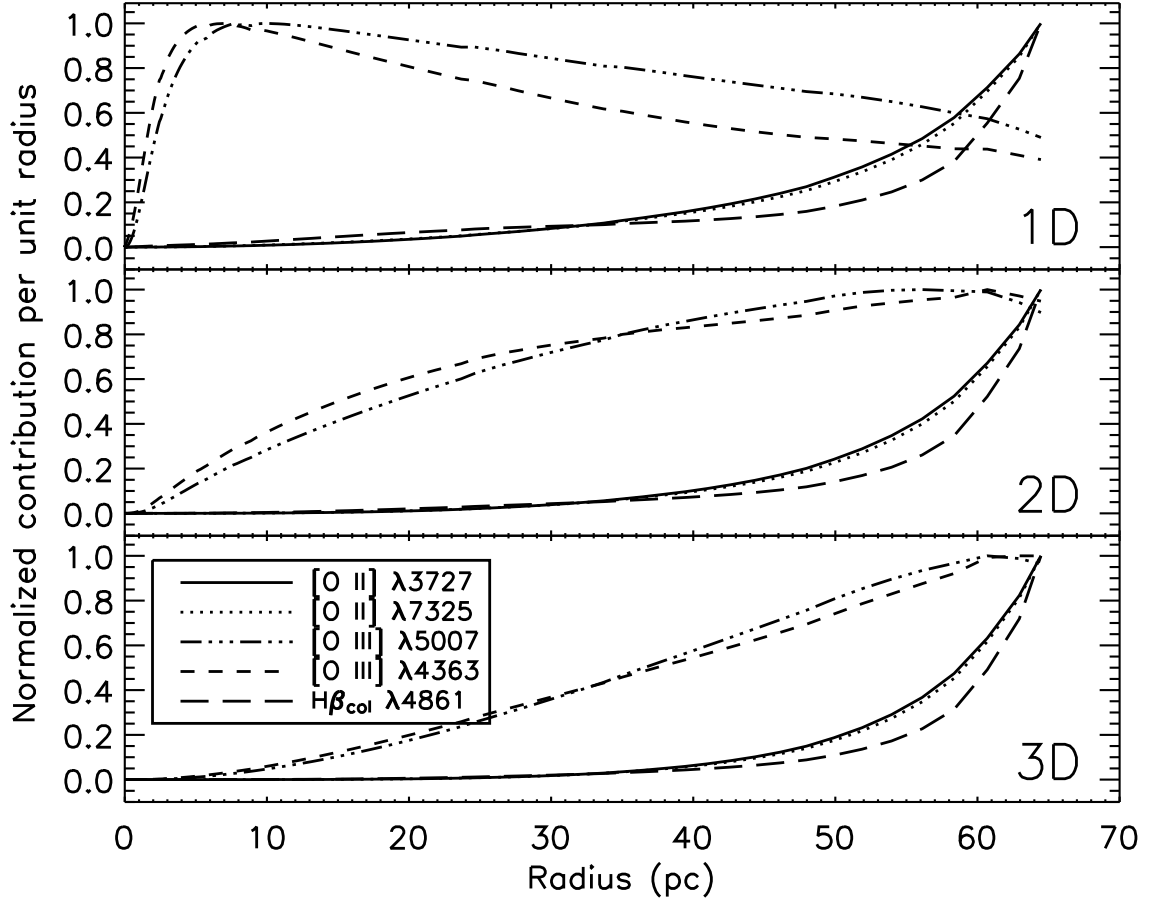


Fig. 1.— Normalized contribution per unit radius to the emission in the main [O II] and [O III] lines and in $H\beta_{\text{col}}$ in a model for NGC 346, showing that $H\beta_{\text{col}}$ preferentially forms in the [O II] zone. The values are normalized to the maximum value in each line. The three panels correspond to different integrations, simulating a beam, a narrow slit, and a slit covering the whole object respectively.

According to this criterion, the fitting philosophy was changed to grant agreement with the [O II] rather than the [O III] temperature. The models of Haro 29 and I Zw 18 used to this aim are the corresponding best-fit models of Paper II, which already fitted the observed $T[\text{O II}]$ temperatures. For SBS 0335 we used model A of Luridiana et al. (2003), which correctly fits the [O II] temperature, instead of the hotter model B, which fits the [O III] temperature and was used in Paper II. For NGC 346 and NGC 2363 (for which in Paper II we only gave estimates based on models compiled from the literature) we computed two new models with Cloudy (version 06.02): the one for NGC 346 is based on model L4 by Relaño et al. (2002), and the one for NGC 2363 is based on the best-fit model for this region by Luridiana et al. (1999). In all the models, the updated collisional rates by Anderson et al. (2000, 2002) were used, and the appropriate corrections for the slit aperture used in the observations were made.

2.4. Resulting estimates of collisional contribution to the Balmer lines

The models described in Sections 2.3, which incorporate the changes described in sections 2.1 and 2.2, were used to derive estimates for the collisional contributions. The results are listed in Table 1. Based on these values, we recalculated the breakdown of $C(\text{H}\beta)^{obs}$ in terms of collisional and dust reddening for the objects of the sample. The results are listed in Table 2. The x_α and x_β values predicted by our model A for SBS 0335 were not published in Paper II.

The effect of using the new atomic data is an increase in the estimated collisional contribution to the Balmer lines. This increase is partially offset by the lower temperature of the photoionization models used in this work: some of the models used in Paper II, computed to fit the observed $T[\text{O III}]$ values, produced $T[\text{O II}]$ values larger by up to 700 K than the observed values, while the new models correctly fit the $T[\text{O II}]$ temperature, and have correspondingly lower collisional rates. In Table 1 we list the new estimates of x_α and x_β and the values of $T[\text{O II}]$.

Table 1. Collisional contribution to the total Balmer intensities^a.

Object	T_e (O II)	Paper II		This work	
		x_α	x_β	x_α	x_β
NGC 346	12600	0.015	0.004	0.011	0.007
NGC 2363	13800	0.030	0.008	0.037	0.027
Haro 29	14000	0.028	0.007	0.033	0.021
SBS 0335-052 ^b	15600	0.074	0.021	0.086	0.066
I Zw 18	15400	0.060	0.017	0.070	0.053

^a $x_\lambda = I(\lambda)_{col}/I(\lambda)_{tot}$ is the ratio between the collisional and the total intensity, calculated with the updated collisional coefficients by Anderson et al. (2000, 2002) for the photoionization models described in Luridiana et al. (1999), Relaño et al. (2002), and Paper II.

^bPredictions of model A for the centermost 1.8'' x 1'' region, corresponding to the sum of the three brightest positions observed by Izotov et al. (1999).

Table 2. Observed, collisional, and collision-corrected reddening coefficients^a.

Object	$C(\text{H}\beta)^{obs}$	Paper II		This work	
		$C(\text{H}\beta)^{col}$	$C(\text{H}\beta)^{dust}$	$C(\text{H}\beta)^{col}$	$C(\text{H}\beta)^{dust}$
NGC 346	0.15 ± 0.01	0.02 ± 0.02	0.13 ± 0.02	0.00 ± 0.00	0.15 ± 0.01
NGC 2363	0.11 ± 0.02	0.03 ± 0.02	0.08 ± 0.02	0.01 ± 0.01	0.10 ± 0.02
Haro 29	0.00 ± 0.08	0.03 ± 0.02	-0.03 ± 0.08	0.02 ± 0.01	-0.01 ± 0.08
SBS 0335-052	0.24 ± 0.02	0.07 ± 0.05	0.17 ± 0.06	0.03 ± 0.01	0.21 ± 0.02
I Zw 18	0.02 ± 0.02	0.06 ± 0.02	0.04 ± 0.02	0.02 ± 0.01	0.00 ± 0.02

^aThe uncertainty in $C(\text{H}\beta)^{col}$ was calculated as in Paper II.

3. Abundance determinations

3.1. Adopted line intensities

In Tables 3 and 4 we present the observed line intensity ratios of the He I lines relative to $H(\beta)$, $F(\lambda)/F(H\beta)$, for the 5 objects without correction for underlying absorption.

Table 3. Adopted He I line intensities relative to $H\beta^a$

He I line	NGC 346 ^b		NGC 2363 ^c		Haro 29 ^c	
	F	I	F	I	F	I
3820	0.011±0.001	0.014±0.001	0.007±0.001	0.010±0.001
3889	0.1820±0.0017 ^d	0.0988±0.0019	0.174±0.001 ^d	0.095±0.003	0.186±0.001 ^d	0.097±0.001
4026	0.0171±0.0006	0.0203±0.0007	0.015±0.001	0.020±0.001	0.016±0.001	0.019±0.001
4387	0.0045±0.0002	0.0054±0.0002	0.004±0.001	0.005±0.001	0.004±0.001	0.005±0.001
4471	0.0370±0.0005	0.0396±0.0005	0.038±0.001	0.042±0.001	0.037±0.001	0.040±0.001
4922	0.0100±0.0002	0.0109±0.0002	0.012±0.001	0.013±0.001	0.009±0.001	0.010±0.001
5876	0.1143±0.0013	0.1075±0.0012	0.112±0.001	0.110±0.002	0.103±0.001	0.105±0.001
6678	0.0336±0.0002	0.0305±0.0002	0.031±0.001	0.030±0.001	0.029±0.001	0.030±0.001
7065	0.0243±0.0002	0.0218±0.0002	0.032±0.001	0.030±0.001	0.025±0.001	0.026±0.001
7281	0.0073±0.0004	0.0066±0.0003	0.006±0.001	0.006±0.001	0.005±0.001	0.005±0.001

^aThe F values and their errors are those presented by the observers. The I values denote the intrinsic fluxes after correcting for underlying absorption, collisional contribution to the Balmer lines, and interstellar reddening; the errors attached to the I values are only those due to the flux errors, see text.

^b F values for region A from Peimbert et al. (2000).

^c F values from Izotov et al. (1997).

^dIncluding the contribution due to H8.

Table 4. Adopted He I line intensities relative to $H\beta^a$

He I line	SBS 0335-52 ^b		I Zw 18 ^c	
	F	I	F	I
3889	0.1606 ± 0.0018^d	0.0948 ± 0.0026	0.1570 ± 0.0043^d	0.0844 ± 0.0052
4026	0.0122 ± 0.0005	0.0179 ± 0.0007	0.0151 ± 0.0036	0.0222 ± 0.0053
4471	0.0339 ± 0.0007	0.0401 ± 0.0008	0.0352 ± 0.0025	0.0412 ± 0.0029
4922	0.0077 ± 0.0004	0.0094 ± 0.0005
5876	0.1168 ± 0.0014	0.1132 ± 0.0014	0.0968 ± 0.0028	0.1016 ± 0.0029
6678	0.0322 ± 0.0005	0.0297 ± 0.0005	0.0273 ± 0.0019	0.0290 ± 0.0020
7065	0.0453 ± 0.0007	0.0406 ± 0.0006	0.0249 ± 0.0016	0.0263 ± 0.0017

^aThe F values and their errors are those presented by the observers. The I values denote the intrinsic fluxes after correcting for underlying absorption, collisional contribution to the Balmer lines, and interstellar reddening; the errors attached to the I values are only those due to the observed flux errors, see text.

^b F values for the three brightest positions by Izotov et al. (1999): center, $0''.05W$, and $0''.6NE$.

^c F values for the southeast region by Izotov et al. (1999).

^dIncluding the contribution due to H8.

To correct for the stellar underlying absorption in the He I and H I lines we made use of synthetic models and observations. The intensity of $H\beta$ was corrected taking into account the observed $H\beta$ equivalent widths in emission, $EW_{em}(H\beta)$, and the $H\beta$ equivalent widths, $EW_{ab}(H\beta)$, based on the models by González Delgado et al. (1999, 2005) (Table 5). The EW_{ab} for the remaining Balmer lines and the He I lines were obtained also from the models by González Delgado et al. (1999, 2005) and Cerviño (private communication), consistently with the adopted $EW_{ab}(H\beta)$ values. The He I $\lambda\lambda$ 7065 and 7281 Å lines are not included in the models by González Delgado et al. (2005), therefore we made use of the observations by Leone & Lanzafame (1998) to correct for the stellar underlying absorption of these lines.

After correcting for the underlying absorption and the collisional contribution to the Balmer lines presented in Table 1, we determined the He I intensities (due to recombinations and collisions, and affected by optical depth effects) relative to the pure recombination $H\beta$ line intensities uncorrected for reddening, $G(\text{He I})/G(H\beta)$. Once these two corrections were made, we combined the $C(H\beta)^{\text{dust}}$ value with the reddening law by Seaton (1979, hereafter S79) and derived the reddening corrected $I(\text{He I})/I(H\beta)$ line intensity ratios; note that $I(H\beta)$ represents the recombination contribution only, while the $I(\text{He I})$ values include recombination and collisional contributions as well as optical depth effects.

In Tables 3 and 4 we present the $I(\text{He I})/I(H\beta)$ line intensity ratios and the errors associated with the observational measurements only; specifically, errors associated with underlying absorption, collisional contribution to the Balmer lines, and interstellar reddening are not included; they will be included in section 3.3 and discussed in section 3.4. We decided to follow this procedure because the maximum likelihood method (MLM) used in section 3.2 to determine the helium physical conditions, requires the errors presented for each line to be independent from each other; while the effects of the uncertainties, from any one of these three sources (underlying absorption, collisional contribution to the Balmer lines, and interstellar reddening), affect the $I(\text{He I})/I(H\beta)$ ratios in a correlated way.

For SBS 0335-052 we used the observed F values by Izotov et al. (1999). We did not use the data presented by Izotov et al. (2006) for the brightest $1''.56 \times 1''.04$ region for this object because, even if the signal to noise is very high, the observations were obtained in seven different spectral ranges which did not correspond exactly to the same region of the sky, this fact renders these observations useless to determine a very accurate Y value (Izotov et al. 2006). We also did not use the data for the whole object by Izotov et al. (2006) because the quality of the line intensity determinations is considerably lower than the quality of the data presented by Izotov et al. (1999).

In Paper I the NGC 346 observations were not corrected for underlying absorption in the He I and H I lines because in region A the bright O stars that ionize the H II

region were avoided. We consider that this decision was incorrect and that most of the continuous emission in region A is due to dust-scattered light showing the He I and H I lines in absorption. The reasons are the following: a) O’Dell & Hubbard (1965), and O’Dell et al. (1966) showed that most of the non-stellar continuum observed in the visual range of the spectrum of H II regions, when the brightest stars are not included in the observing slit, is due to dust-scattered light, b) comparing the equivalent width of region A, $EW(H\beta) = 250 \text{ \AA}$, to the expected $EW(H\beta)$ for a low density plasma at 12500 K, which amounts to $\sim 1230 \text{ \AA}$ (e.g. Aller 1984; Osterbrock & Ferland 2006, and references therein), it is found that about 80% of the continuum light is not produced by the nebular gas, c) The color of the underlying spectrum obtained by subtracting the nebular continuum from the observed spectrum is bluer than that provided by OB stars and therefore cannot be due to A and later type stars (the intensity of the observed continuum at different wavelengths can be obtained from the EW of the emission lines presented in Table 5 of Peimbert et al. (2000), and the absolute line intensities presented in Table 2 of the same paper; the intensity of the nebular continuum at different wavelengths can be obtained from Table 4-9 by Aller (1984) and the intensities at different wavelengths for stars of different spectral types can be obtained from Table 8 of the paper by Code (1960)). Since the OB stars were avoided from the observations, it can neither be due to them. We conclude from the previous arguments that most of the underlying continuum in region A of NGC 346 is due to dust-scattered light provided by the brightest OB stars of the cluster.

3.2. The Y determinations

The abundance analysis of these objects is based on the combined use of standard empirical relations and tailored photoionization models. For NGC 2363, we used the models described in Luridiana et al. (1999), while for NGC 346 we used the model by Relaño et al. (2002). As mentioned in Section 2, the models for the remaining three objects were presented in Paper II.

In addition to the collisional contribution to the Balmer lines, to obtain He^+/H^+ values we need a set of effective recombination coefficients for the helium and hydrogen lines, an estimate of the optical depth effects for the He I lines, and the contribution to the He I line intensities due to collisional excitation. We used the hydrogen recombination coefficients by Storey & Hummer (1995), the helium recombination coefficients by Porter et al. (2005), with the interpolation formulae provided by Porter et al. (2007), and the collisional contribution to the He I lines by Sawey & Berrington (1993) and Kingdon & Ferland (1995). The optical depth effects in the triplet lines were estimated from the computations by

Benjamin, Skillman, & Smits (2002).

As in Paper I, we used a maximum likelihood method (MLM) based on the He I line intensities to derive the $N(\text{He}^+)/N(\text{H}^+)$ values. We produced two sets of models, one where we assumed constant temperature ($t^2 = 0.000$), given by $T(4363/5007)$, and obtained τ_{3889} , n_e , and $N(\text{He}^+)/N(\text{H}^+)$, and the other set of models where $T(\text{He}^+)$ was an additional variable determined also by the MLM, in all cases $T(\text{He}^+)$ resulted smaller than $T(4363/5007)$, to reconcile both temperatures it is necessary to assume the presence of temperature variations characterized by ($t^2 \neq 0.000$) (see Peimbert (1967) and Paper I). The resulting values are presented in Table 5, where the errors include only those due to: the temperature structure, the density structure, the optical depth of the He I triplet lines, and the adopted line intensities.

The MLM solutions with $t^2 \neq 0.000$ yield lower values of $N(\text{He}^+)/N(\text{H}^+)$ than those with $t^2 = 0.000$ (see Table 5). This change is not due to the variation of the He I recombination coefficients with temperature, which in this range of temperature is very small. The change is mainly due to the higher densities, derived from the MLM when $t^2 \neq 0.000$, which increase the importance of the collisional excitation of the He I lines. The densities for $t^2 \neq 0.000$ of the whole sample are about 67 cm^{-3} higher than for $t^2 = 0.000$. The MLM densities for NGC 346 and Haro 29 are 4 ± 15 and $-7 \pm 50 \text{ cm}^{-3}$ respectively, these values are too low and support the idea that t^2 has to be larger than 0.000. In Table 5 we have adopted for NGC 346 and Haro 29 a density of 10 cm^{-3} for $t^2 = 0.000$. The rms density for NGC 346 is $14 \pm 3 \text{ cm}^{-3}$ (Peimbert et al. 2000), a reasonable value for this type of objects. The rms density is the minimum density that can be associated to an H II region. For real nebulae, which always present large density variations, the local density associated with the physical mechanisms that produce the line intensities, is always considerably higher than the rms density (e.g. Osterbrock & Flather 1959; Peimbert 1966).

The total helium to hydrogen abundance ratio was derived using the following equation

$$\begin{aligned} \frac{N(\text{He})}{N(\text{H})} &= \frac{\int N_e N(\text{He}^0) dV + \int N_e N(\text{He}^+) dV + \int N_e N(\text{He}^{++}) dV}{\int N_e N(\text{H}^0) dV + \int N_e N(\text{H}^+) dV}, \\ &= ICF(\text{He}) \frac{\int N_e N(\text{He}^+) dV + \int N_e N(\text{He}^{++}) dV}{\int N_e N(\text{H}^+) dV}, \end{aligned} \quad (3)$$

where $ICF(\text{He})$ is the helium ionization correction factor. The $ICF(\text{He})$ values were obtained from the Cloudy models and are presented in Table 5. To obtain the $N(\text{He}^{++})/N(\text{H}^+)$ values, we used the $I(4686)/I(\text{H}\beta)$ value together with the recombination coefficients by Brocklehurst (1971).

Table 5. Physical Parameters for the H II Regions

	NGC 346	NGC 2363	Haro 29	SBS 0335-052 ^a	I Zw 18
$EW_{em}(\text{H}\beta)$	250 ± 10	187 ± 10	224 ± 10	169 ± 10	135 ± 10
$EW_{abs}(\text{H}\beta)$	2.0 ± 0.5	2.0 ± 0.5	2.0 ± 0.5	2.0 ± 0.5	2.9 ± 0.5
$ICF(\text{He})$	1.000 ± 0.001	0.993 ± 0.001	0.9955 ± 0.001	0.991 ± 0.001	1.000 ± 0.001
$n_e(t^2 = 0.000)$	10 ± 15	205 ± 67	10 ± 50	230 ± 41	57 ± 70
$\tau_{3889}(t^2 = 0.000)$	0.10 ± 0.20	1.12 ± 0.40	1.65 ± 0.29	2.65 ± 0.35	0.06 ± 0.05
$N(\text{He}^+)/N(\text{H}^+)(t^2 = 0.000)^b$	8506 ± 48	8570 ± 175	8651 ± 162	8542 ± 146	8451 ± 354
$N(\text{He})/N(\text{H})(t^2 = 0.000)^b$	8528 ± 50	8584 ± 176	8710 ± 163	8757 ± 147	8522 ± 354
$N(\text{O})/N(\text{H})(t^2 = 0.000)^b$	11.5 ± 1.8	8.88 ± 0.82	7.43 ± 0.75	2.26 ± 0.25	1.66 ± 0.17
$O(t^2 = 0.000)^c$	139 ± 22	107 ± 10	89 ± 9	27 ± 3	20 ± 2
t^2	0.019 ± 0.008	0.021 ± 0.011	0.024 ± 0.008	0.040 ± 0.010	0.025 ± 0.006
$n_e(t^2 \neq 0.000)$	58 ± 33	285 ± 92	61 ± 50	329 ± 61	90 ± 80
$\tau_{3889}(t^2 \neq 0.000)$	0.10 ± 0.20	1.04 ± 0.40	1.28 ± 0.30	2.56 ± 0.35	0.06 ± 0.05
$N(\text{He}^+)/N(\text{H}^+)(t^2 \neq 0.000)^b$	8372 ± 77	8425 ± 180	8453 ± 172	8273 ± 158	8297 ± 346
$N(\text{He})/N(\text{H})(t^2 \neq 0.000)^b$	8399 ± 79	8440 ± 181	8513 ± 173	8490 ± 159	8368 ± 346
$N(\text{O})/N(\text{H})(t^2 \neq 0.000)^b$	13.5 ± 2.0	10.7 ± 0.8	8.85 ± 1.00	3.26 ± 0.33	2.16 ± 0.25
$O(t^2 \neq 0.000)^c$	163 ± 25	129 ± 10	106 ± 12	39 ± 4	26 ± 3

^aValues for the three brightest positions by Izotov et al. (1999).

^bIn units of 10^{-5} .

^cOxygen abundance by mass, in units of 10^{-5} .

From the normalization by unit mass given by $X + Y + Z = 1$, the $N(\text{He})/N(\text{H})$ values, the $N(\text{O})/N(\text{H})$ values, and the assumption that the oxygen by mass, O , amounts to $55\% \pm 10\%$ of the Z value, it is possible to derive Y and O . The $N(\text{O})/N(\text{H})$ and O values are presented in Table 5, while the Y values are presented in Table 6.

The $O/Z = 0.55 \pm 0.10$ value was derived by extrapolating to $O = 0$ the O/Z values for the Orion nebula, 30 Doradus in the LMC, and NGC 346 in the SMC derived by Peimbert (2003), which amount to $(43 \pm 5)\%$, $(46 \pm 7)\%$, and $(53 \pm 8)\%$, respectively. Note that NGC 346 is the O richest object in our sample and that the increase in the O fraction with decreasing Z is mainly due to the decrease of the C/O and N/O ratios with decreasing O abundance. The error in the O/Z ratio translates into an error slightly smaller than 0.0001 in the Y_p determination.

The O values in Table 5 are slightly different to those presented in Paper I due to four causes: a) the $N(\text{O})/N(\text{H})$ values are higher because we took into account the collisional contribution to the Balmer line intensities, b) the $N(\text{He})/N(\text{H})$ ratios are higher, c) the t^2 values are slightly different, because the adopted line intensities are slightly different, and d) we assumed that 10% of the O atoms are trapped in dust grains in all objects.

In Table 6 we explicitly present the ΔY increase due to the collisional excitation of the Balmer lines. Also in this table we present the Y values for $t^2 = 0.000$ and those derived for $t^2 \neq 0.000$. The Y and Y_p values present first the statistical and then the systematic errors from all the sources presented in Table 7 (note that the $N(\text{He})/N(\text{H})$ ratios presented in Table 5 only include a subset of the statistical errors, those due to: temperature structure, density structure, optical depth effects and line intensities). For each object we determine a Y_p value and at the end of the table we present the Y_p value for the whole sample, $Y_p(\text{sample})$. The error budget for the $Y_p(\text{sample})$ is discussed in the error budget subsection.

3.3. The Y_p determination

To determine the Y_p value from all the objects it is necessary to estimate the fraction of helium present in the interstellar medium produced by galactic chemical evolution. We will assume that

$$Y_p = Y - O \frac{\Delta Y}{\Delta O}, \quad (4)$$

where O is the oxygen abundance by mass. From chemical evolution models of different galaxies it is found that $\Delta Y/\Delta O$ depends on the initial mass function, the star formation rate, the age, and the O value of the galaxy in question. But $\Delta Y/\Delta O$ is well fitted by a constant value for objects with the same IMF, the same age, and an O abundance smaller

than $\sim 4 \times 10^{-3}$ (Peimbert et al. 2007). Consequently in what follows we will adopt a constant value for $\Delta Y/\Delta O$.

The $\Delta Y/\Delta O$ value derived by Peimbert et al. (2000) from observational results and models of chemical evolution of galaxies amounts to 3.5 ± 0.9 . More recent results are those by Peimbert (2003), who finds 2.93 ± 0.85 from observations of 30 Dor and NGC 346, and by Izotov et al. (2006) who find $\Delta Y/\Delta O = 4.3 \pm 0.7$ from the observations of 82 H II regions. We have recomputed the Izotov et al. value considering two systematic effects not considered by them: the fraction of oxygen trapped in dust grains, which we estimate to be 10%, and the increase in the inferred O abundances due to the presence of temperature fluctuations, which for this type of H II regions we estimate to be about 0.08 dex (Relaño et al. 2002). From these considerations we obtain $\Delta Y/\Delta O = 3.2 \pm 0.7$. On the other hand Peimbert et al. (2007) from chemical evolution models with different histories of galactic inflows and outflows for objects with $O < 4 \times 10^{-3}$ find that $2.4 < \Delta Y/\Delta O < 4.0$. From the theoretical and observational results we have adopted a value of $\Delta Y/\Delta O = 3.3 \pm 0.7$, which we have used with the Y and O determinations from each object to obtain the set of Y_p determinations presented in Table 6.

To determine the Y_p average from the whole sample we first need to find the weight that should be assigned to each object by considering the confidence we have in each one of the determinations. For this we added in quadrature the errors provided by the MLM, presented in Table 5, plus all the additional sources of error presented in Table 7, with the exception of the errors associated with the recombination coefficients of both H and He (which will affect the sample as a whole and thus will not affect the relative confidence we have in the determination from each object). The quadratic addition of these 11 sources of error result in: $err_{\Sigma 11}(\text{NGC 346})=0.00311$, $err_{\Sigma 11}(\text{NGC 2363})=0.00507$, $err_{\Sigma 11}(\text{Haro 29})=0.00475$, $err_{\Sigma 11}(\text{SBS 0335-052})=0.00583$, and $err_{\Sigma 11}(\text{I Zw 18})=0.00867$. And the weights obtained in this way, for each object in the sample, amount to: $w(\text{NGC 346})=0.4515$, $w(\text{NGC 2363})=0.1697$, $w(\text{Haro 29})=0.1927$, $w(\text{SBS 0335-052})=0.1281$, and $w(\text{I Zw 18})=0.0579$.

We use these weights to determine the different helium averages $\langle Y \rangle = \sum_i Y(i)w(i)$ along with the corresponding statistical errors $err_{sta} = (\sum_i [err_{sta}(i)w(i)]^2)^{1/2}$ and systematic errors $err_{sys} = \sum_i err_{sys}(i)w(i)$; finally we add the statistical and systematic errors in quadrature.

To compare our results with those of other authors that assume $t^2 = 0.000$ we have computed $Y_p(t^2 = 0.000) = 0.2523 \pm 0.0027$, using the five Y and O values for $t^2 = 0.000$ presented in Tables 5 and 6, note that this value is not presented in Table 6. Also, from the five Y_p values for $t^2 \neq 0.000$ presented in Table 6, we derive $Y_p = 0.2477 \pm 0.0029$.

Table 6. Y and Y_p values

	$\Delta Y(\text{Hc})^b$	Y $t^2 = 0.000$	Y $t^2 \neq 0.000$	Y_p^a $t^2 \neq 0.000$
NGC 346	0.0015 ± 0.0005	0.2537	$0.2507 \pm 0.0027 \pm 0.0015$	$0.2453 \pm 0.0027 \pm 0.0019$
NGC 2363	0.0057 ± 0.0016	0.2551	$0.2518 \pm 0.0047 \pm 0.0020$	$0.2476 \pm 0.0047 \pm 0.0022$
Haro 29	0.0047 ± 0.0013	0.2577	$0.2535 \pm 0.0045 \pm 0.0017$	$0.2500 \pm 0.0045 \pm 0.0019$
SBS 0335–052	0.0144 ± 0.0038	0.2594	$0.2533 \pm 0.0042 \pm 0.0042$	$0.2520 \pm 0.0042 \pm 0.0042$
I Zw 18	0.0114 ± 0.0031	0.2529	$0.2505 \pm 0.0081 \pm 0.0033$	$0.2498 \pm 0.0081 \pm 0.0033$
Sample	0.0056 ± 0.0015	0.2554	$0.2517 \pm 0.0018 \pm 0.0021$	$0.2477 \pm 0.0018 \pm 0.0023^c$

^aDerived from each object under the assumption that $\Delta Y/\Delta O = 3.3 \pm 0.7$ see text.

^bIncrease in the Y abundance due to the collisional contribution to the Balmer line intensities.

^cEqual to 0.2477 ± 0.0029 .

3.4. The error budget

Based on the errors presented in Table 5 and Table 6, and the discussion in this subsection, we have elaborated the error budget for the whole sample of our Y_p determination and it is presented in Table 7. The errors in the table are grouped in discrete bins because they represent broad estimates. In this table the sources of error are listed in order of importance, we will say a few words for some of them. The error budgets of other Y_p determinations are different to ours for many reasons, they depend on the sample of H II regions and on the treatment given by the different groups to each source of error.

It is difficult to estimate the magnitude of the Y_p error caused by each of the thirteen sources of error, since there is a significant interdependence between some of them; for instance, the uncertainty in the hydrogen collisions will modify the reddening determination for each object. To quantify the total effect of each source of error in the Y_p determination we used the following approach: a) we started with the four errors derived from the MLM (He I and H I line intensities, optical depth of the He I triplet lines, collisional excitation of the He I lines due to the average density, and temperature structure); b) we ordered the other sources of error to be considered one at a time (in order: density structure, helium *ICF*, underlying absorption of the H I and He I lines, reddening correction, collisional excitation of the H I lines, O ($\Delta Y/\Delta O$) correction, and recombination coefficients of the H I and He I lines); c) we measured how a change in each source affects the determination of all the previous quantities; d) we presented the total amount as the estimated contribution to the Y_p error for this latest source, thus all the cross correlations with the previous sources of error are included in the later source. For example, the Y_p error produced by the modification of the reddening correction due to the hydrogen collisions is presented as part of the error due to the hydrogen collisions, and is not presented as part of the error due to the reddening correction; also not presented, is the increase in the $C(\text{H}\beta)$ formal error due to the uncertainty of the hydrogen collisions determinations.

Estimated in this manner each source of error is independent from the others, even the ones labeled as systematic. Consequently the standard deviation of the total error is computed by adding in quadrature the standard deviation of all the sources of error. Note that we are not assuming that any of the thirteen errors has a normal distribution (even if several of the error distributions probably are normal), we are reporting what we estimate to be the standard deviation of the Y_p error due to each source; also, with thirteen independent sources of error included, we expect the final error to be close to a normal distribution.

In Table 7 we have divided the sources of error in two groups, statistical and systematic. The errors labeled as statistical will affect differently the Y_p determination for each object; therefore, increasing the number of objects in the sample will reduce their final magnitude.

On the other hand the errors labeled as systematic, are so in the sense that for any one of them our lack of understanding shifts the Y_p determination of each object in the same direction, for some of them by different amounts, producing an error in the determination that cannot be reduced by simply increasing the number of objects; for some of them the error can be diminished by selecting a small group of objects where we expect this effect to be minimum. The specific equations that should be used to determine the errors from a sample, which differentiate the treatment given to the systematic and statistical errors, are presented in the fourth paragraph of section 3.3 and were used to estimate the final error of the Y_p determination.

As expected the total error obtained from Table 7 is in agreement with the total error presented in Table 6 and implies that the estimates of the different sources of errors in both tables are equivalent.

The most important source of error in the determination of Y_p is the collisional excitation of the Balmer lines. The collisional contribution to the Balmer lines produces a non-negligible increase in the Balmer line intensities relative to the case B recombination and could introduce a bias in the reddening correction deduced from the observed $H\alpha/H\beta$ ratio, both effects affecting the Y determination. For our sample the Balmer collisional contribution on the reddening correction is practically negligible (see Table 2). On the other hand the collisional contribution to the Balmer line intensities is very important in the Y determination (see Table 6). We will give an approximate estimate of the error introduced by this effect on our Y_p determination. We will consider three sources of error: the collisional rates, the radiative cascade, and the model fitting (see section 2). The published collisional rates are expected to become increasingly accurate with time, and the current uncertainty on them, estimated from the variation of the Ω s published in the last decade, is of the order of 15% for $\Omega(1s, 3)$ and $\Omega(1s, 4)$ in the temperature range of interest to us. These values translate into almost identical values for $I(H\alpha_{\text{col}})$ and $I(H\beta_{\text{col}})$, which in turn would correspond to an uncertainty of about 0.0009 in Y_p . The errors on the assumed path for the radiative cascade are negligible, since the breakdown of a given $\Omega(1s, n)$ among sublevels is much less uncertain than the absolute value of the $\Omega(1s, n)$ itself. On the other hand, model fitting of the observed H II region is the leading source of uncertainty, because the ionization and temperature structures are difficult to constrain to the high level of accuracy that would be desirable given the strong dependence of the collisional rates on the electron temperature and the neutral hydrogen fraction. In Section 2, we have shown that the collisional contribution to the Balmer lines mostly comes from the region where the [O II] lines originate, so that it is important for a good model to reproduce the observed $T[\text{O II}]$ temperature. Our estimate of the uncertainty is based on the range covered by the collisional contribution in models that acceptably fit the $T[\text{O II}]$ temperature. By comparing reasonable photoionization models

for the same object we consider that the model fitting introduces an error of about 22% on the collisional contribution to the Balmer lines. The combination of the three sources of error amounts to about 27% of the collisional contribution to the Balmer lines of our sample, which translates into an error of about 0.0015 in Y_p .

We consider the error associated with the collisional excitation of the H I lines as systematic because this process has not been studied at length by different groups, hence this effect could be systematically lower or higher for all the objects. The error might become statistical once the problem is studied further, but in any case we expect it to depend strongly on the photoionization models needed for its estimation.

The second most important source of error is the temperature structure. Most Y determinations are based on $T(4363/5007)$, but other temperature determinations yield lower values, and photoionization models do not predict the high $T(4363/5007)$ values observed. These results indicate the presence of temperature variations which should be included in the Y determination (see Paper I). The best procedure to take into account the temperature structure is to determine $T(\text{He}^+)$ based on the maximum likelihood method. The Y abundances derived from $T(\text{He}^+)$ are typically lower by about 0.0040 than those derived from $T(4363/5007)$. The error quoted in Table 7 is due to the error in the $T(\text{He}^+)$ determinations obtained with the MLM (see section 3.2). The difference between both temperatures is not correlated to the metallicity of the H II region, therefore the systematic error introduced by the use of $T(4363/5007)$ in the Y determination is similar for objects with different metallicities.

We have estimated the error in the Y_p determination due to the adopted effective recombination coefficients based on the confidence in the He I line emissivities presented by Bauman et al. (2005). The lines used to determine the helium abundances are $\lambda\lambda$ 3820A, 3889B, 4026AA, 4387A, 4471A, 4921A, 5876A, 6678A, 7065A, and 7281A, where the letter indicates the confidence: AA better than 0.1%, A in the 0.1 to 1% range, and B in the 1 to 5% range. From these values we estimate a systematic error due to the computed emissivities of about 0.0010 in Y . According to Porter et al. (2007), the error introduced in the emissivities by interpolating the equations provided by them in temperature is smaller than 0.03%, which translates into an error in Y_p considerably smaller than 0.0001. In our preliminary estimate of Y_p (Peimbert et al. 2007) we used a different interpolation to the Porter et al. (2005) He I atomic recombination coefficients than that given by Porter et al. (2007), as well as a slightly different error budget, and obtained that $Y_p = 0.2474 \pm 0.0028$.

The third most important source of error is the extrapolation to zero heavy elements content. Fortunately, based on chemical evolution models of galaxies of different types, it is found that $\Delta Y/\Delta O$ is practically constant for objects with $O < 4 \times 10^{-3}$, and in good

agreement with the observational determinations (see the previous section). One of the sources of error in the observational determination is the fraction of oxygen trapped in dust grains which has to be taken into account.

As was demonstrated by Olive & Skillman (2004), the reddening correction is an important source of error. Therefore to estimate the error in the reddening correction we will make comparisons among three classic extinction laws and a recent one, these laws are labeled: S79, W58 (Whitford 1958; as parameterized by Miller & Mathews 1972), CCM89 (Cardelli et al. 1989), and B07 (Blagrove et al. 2007). Fortunately, for our sample the average $C(H\beta)$ value amounts to 0.09 only, see Table 2. For the 4500 to 7300 Å region the differences among the S79, W58 and CCM89 extinction laws produce differences in the $I(He\lambda)/I(H\beta)$ values of our sample of about 0.15%, which correspond to an average difference smaller than 0.0002 in the final Y_p determination. For the 3800 to 4400 Å region the differences between S79 and W58 produce differences of about 0.4% in the line intensity ratios, which, when combined with all the He I lines available, correspond to differences smaller than 0.0004 on Y_p . For the 3800 to 4400 Å region the use of the CCM89 law for $R_V = 3.16$, instead of the S79 law used by us, gives systematically higher $I(He\lambda)/I(H\beta)$ values by about 1%, increasing Y_p by about 0.0008 relative to our result when all the He I lines presented in Table 3 and Table 4 are used. Cardelli et al. (1989) made a strong effort to find a simple analytical law to be useful for all R_V values, we consider that in the 3800 to 4400 Å range the CCM89 law might overestimate the extinction because it might not be perfectly represented by a seventh order polynomial. Support for this idea comes from Blagrove et al. (2007), who find that the CCM89 law for $R_V = 5.5$ overestimates the extinction in the 3030 to 4350 Å region when compared with the B07 law. The B07 extinction law is intended to reproduce the Orion reddening law using a modified CCM89 extinction ($R_V = 5.5$) which only differs from the CCM89 one in the 3030 to 4350 Å region. Based on the previous discussion we estimate that the error in the Y_p determined by us due to the reddening correction amounts to about 0.0007 and we consider that most of this error is systematic. Note that for a sample with an average $C(H\beta)$ of 0.2 our estimate of the error in Y_p increases to about 0.0016.

It has often been shown that the correction for underlying absorption in the H I and He I lines has been underestimated (Skillman et al. 1998; Olive & Skillman 2004; Porter et al. 2007). We consider that the best procedure to correct for underlying absorption is to use the models by González Delgado et al. (1999, 2005). According to these models for those objects with $EW_{em}(H\beta) \geq 150\text{Å}$ the expected $EW_{ab}(H\beta)$ amounts to $\approx 2\text{Å}$; for objects with $EW_{em}(H\beta) \leq 150\text{Å}$ (older objects), the expected $EW_{ab}(H\beta)$ becomes larger. Therefore the correction for underlying absorption for objects with $EW_{em}(H\beta) \geq 150\text{Å}$ is inversely proportional to $EW_{em}(H\beta)$, while for objects with $EW_{em}(H\beta) \leq 150\text{Å}$ the correction, and consequently the associated error, increases even faster due to the larger $EW_{ab}(H\beta)$ predicted

by the models. For samples including a large fraction of objects with $EW_{em}(H\beta) \leq 150\text{\AA}$ we expect the error for this concept to be larger than ours, moreover to agree with the models by González Delgado et al. (1999, 2005) the average $EW_{ab}(H\beta)$ for any given sample has to be equal or larger than 2\AA .

In principle, the larger the number of He I lines used to determine a given Y value the better. But there are two additional issues that have to be considered for some of the He I lines that are not included in our determination: a) the accuracy of the atomic data for some of the lines is lower than that for those lines which we have used (Bauman et al. 2005), and b) the radiative transfer of the He I singlet lines has to be taken into account for the $p - s$ and $s - p$ transitions (Robbins & Bernat 1973, 1974).

It is possible that further work might uncover additional sources of systematical errors that would increase the final error. Increasing the sample with objects as well observed as those in our sample and with tailor made photoionization models of similar quality as those used by us will reduce the statistical errors but not the systematic ones. It is also possible that some of the errors that we consider to be dominated by systematics might be reduced by further work, for example by choosing a different set of objects where a particular systematic effect is expected to be lower, or by providing more detailed observations, or by increasing the accuracy of the atomic data determinations, or by providing more realistic models for the observed H II regions.

Table 7. Error budget in the $Y_p(\text{sample})$ determination

Problem	Estimated error
Collisional Excitation of the H I Lines	$\pm 0.0015^b$
Temperature Structure	$\pm 0.0010^a$
$O(\Delta Y/\Delta O)$ Correction	$\pm 0.0010^b$
Recombination Coefficients of the He I Lines	$\pm 0.0010^b$
Collisional Excitation of the He I Lines	$\pm 0.0007^a$
Underlying Absorption in the He I Lines	$\pm 0.0007^a$
Reddening correction	$\pm 0.0007^b$
Recombination Coefficients of the H I Lines	$\pm 0.0005^b$
Underlying Absorption in the H I Lines	$\pm 0.0005^a$
Helium Ionization Correction Factor	$\pm 0.0005^a$
Density Structure	$\pm 0.0005^a$
Optical Depth of the He I Triplet Lines	$\pm 0.0005^a$
He I and H I Line Intensities	$\pm 0.0005^a$

^aStatistical error.

^bSystematic error.

4. Comparison with other Y_p determinations

The difference between our Y_p value of 0.2477 and the 0.2391 value presented in Paper II amounts to 0.0086, and is mainly due to: the change in the He I recombination coefficients (which produced an increase in Y_p of about 0.0040), the change in the H I collisional excitation coefficients (which produced an increase in Y_p of about 0.0025), the correction for underlying absorption in the red He I lines, and the correction of NGC 346 for underlying absorption. In Paper II we used different He I recombination coefficients, those by Smits (1996) and Benjamin, Skillman, & Smits (1999).

It is beyond the scope of this paper to present an error budget for the Y_p determinations of other authors, but we will discuss some of the reasons responsible for the different Y_p values derived by other authors.

There are many differences with respect to the procedure followed by Izotov & Thuan (2004), who derived $Y_p = 0.2421 \pm 0.0021$. At least two of them are systematic: our use of the recent He I recombination coefficients by Porter et al. (2005, 2007), which yield Y values about 0.0040 higher than the previous ones, and our use of the recent H I collisional data (see Section 2), which further increase the Y values over the older H I collisional corrections by about 0.0025.

Olive & Skillman (2004) find a $Y_p = 0.249 \pm 0.009$. Our result is in agreement with theirs, but our error is smaller. Again there are the systematic differences due to the He I recombination data used by both groups and to the estimation of the collisional contribution to the H Balmer lines, these two effects probably would increase their result by about 0.006.

Fukugita & Kawasaki (2006) based on a reanalysis of the Izotov & Thuan (2004) sample of 33 H II regions determined a value of $Y_p = 0.250 \pm 0.004$. In addition to a different treatment of the underlying H and He I absorption there are four systematic effects between their determination and ours. Fukugita & Kawasaki (2006) used the He I recombination data by Benjamin et al. (1999), did not take into account the collisional excitation of the Balmer lines, adopted the $T(4363/5007)$ value instead of the temperature provided by the He I lines to determine Y , and assumed that $ICF(\text{He}) = 1.000$. Including the first two effects would increase their Y_p value by about 0.009, while the consideration of the third effect decreases their determination by about 0.004, the assumption of $ICF(\text{He}) = 1.000$ has to be tested with photoionization models, for our sample three of our models showed $ICF(\text{He})$ values smaller than 1.000. By using our sample as representative of their sample (which might not be true) their Y_p value gets reduced by 0.001. Another problem with their determination is that it implies a decrease of the He I underlying absorption with metallicity, which is not expected; what is expected instead is a decrease of the underlying absorption

with an increase of the equivalent width in emission of $H\beta$.

5. Cosmological implications

To compare our Y_p value with the primordial deuterium abundance D_p (usually expressed as $10^5(D/H)_p$) and with the WMAP results, we will use the framework of the standard big bang nucleosynthesis. The ratio of baryons to photons multiplied by 10^{10} , η_{10} , is given by (Steigman 2006b):

$$\eta_{10} = (273.9 \pm 0.3)\Omega_b h^2, \quad (5)$$

where Ω_b is the baryon closure parameter, and h is the Hubble parameter. In the range $4 \lesssim \eta_{10} \lesssim 8$ (corresponding to $0.2448 \lesssim Y_p \lesssim 0.2512$), Y_p is related to η_{10} by (Steigman 2006a):

$$Y_p = 0.2384 + \eta_{10}/625. \quad (6)$$

In the same η_{10} range, the primordial deuterium abundance is given by (Steigman 2006a):

$$10^5(D/H)_p = D_p = 46.5\eta_{10}^{-1.6}. \quad (7)$$

From our Y_p value, the D_p value by O’Meara et al. (2006), the $\Omega_b h^2$ value by Spergel et al. (2006), and the previous equations we have produced Table 8. From this table, it follows that within the errors the Y_p , D_p , and *WMAP* observations are in very good agreement with the predicted SBBN values.

Table 8. Cosmological predictions based on SBBN and observations.

Method	Y_p	D_p	η_{10}	$\Omega_b h^2$
Y_p	0.2477 ± 0.0029^a	$2.78^{+2.28}_{-0.98}^b$	5.813 ± 1.81^b	0.02122 ± 0.00663^b
D_p	0.2476 ± 0.0006^b	2.82 ± 0.28^a	5.764 ± 0.360^b	0.02104 ± 0.00132^b
<i>WMAP</i>	0.2482 ± 0.0004^b	2.57 ± 0.15^b	6.116 ± 0.223^b	0.02233 ± 0.00082^a

^aObserved value.

^bPredicted value.

6. Discussion

The effect of collisions on the H Balmer spectrum emerges from this work as the leading source of uncertainty for our sample. This uncertainty has in turn three independent sources: the theoretical uncertainty on the collisional Ω s, the incompleteness of the collisional Ω s, and the uncertainty on the physical conditions of the gas at which collisions occur.

The last of these factors is probably the most severe. The collisional excitation of the Balmer lines is stronger in the hotter zones of the H II regions (which are predicted to be the innermost in this metallicity range) and in the less ionized zones (which are the outermost). Since the fraction of neutral hydrogen in a nebula varies over a much wider range than the Boltzmann factor, which is the main temperature dependence of collisions, the contribution of the outer zones dominates, so that $T(\text{O II})$ is the most appropriate temperature to characterize collisions when trying to model them. Additionally, in observations covering a large fraction of the nebula the emitting volume of the outer parts outweighs that of the inner parts, strengthening this conclusion. However, H II regions that are density bounded or have a strongly inhomogeneous temperature structure might escape this rule, particularly when observed with small apertures. In these cases the uncertainty will be larger.

It is clear that only detailed observations and tailored modeling will allow us to reduce the uncertainty introduced by the collisional excitation of the Balmer lines, particularly in the extreme cases; but a better choice might be to avoid critical H II regions altogether, by preferentially selecting those H II regions in which collisions are known in advance to play only a minor role, i.e. objects with moderate temperatures. Since the temperature in H II regions is mostly determined by metallicity, this amounts to saying that metal-poor objects are more adequate than extremely metal-poor objects in Y_P determinations. This conclusion runs counter the common wisdom that the best candidates for primordial helium determinations are extremely metal-poor objects ($Z \lesssim 0.0005$), because they permit to minimize the error introduced by the extrapolation of the (Y, O) relation to $O/H = 0$: although this is true, a larger uncertainty on Y_p is introduced by collisions than the one introduced by most of the other sources, including the slope $\Delta Y/\Delta O$, so the observational efforts should be better directed at metal-poor objects.

Further disadvantages of extremely metal-poor objects in the quest for primordial helium are that their number is very small and that their H II regions are relatively faint. These disadvantages, together with the uncertainty on collisions discussed above, largely outweigh the advantage implied by the smaller error introduced by the extrapolation of the (Y, O) relation to zero metallicity. Therefore, we are led to the strong conclusion that not so extremely metal poor objects, like those in the $0.0005 \lesssim Z \lesssim 0.001$ range, are more appro-

priate for the determination of Y_p : in this range of metallicity it is possible to find a large set of objects with bright H II regions, which will improve the quality and number of emission lines available for the determination of physical conditions; furthermore, the temperatures of these objects are smaller than those of more metal-poor objects and consequently the correction due to the collisional excitation of the H I lines is also smaller.

This conclusion leads us to another critical point in the approach to Y_p . It has been noted that the uncertainty on Y_p is dominated by systematic errors (Olive & Skillman 2004). As long as this is the case, it is preferable to analyze a few objects in depth and try to correct for the systematics than to perform a more shallow analysis of a larger sample, since this last method can reduce the statistical uncertainties but not the systematic errors. Hence we strongly support the methodological choice of understanding as well as possible the details of the objects in a small sample, before directing our efforts towards extending the sample. It is only by means of this approach that systematical errors, such as those arising from the temperature structure of H II regions, can be gradually understood, corrected for, and eventually transformed into statistical uncertainties.

7. Conclusions

The new He I atomic recombination coefficients by Porter et al. (2005, 2007) increase the Y_p determination by about 0.0040 with respect to Paper II.

The H collisional excitation coefficients by Anderson et al. (2000, 2002) increase the Y_p determination by about 0.0025 with respect to Paper II.

The adoption of temperature variations, instead of the assumption of constant temperature given by $T(4363/5007)$, reduces the Y_p determinations by about 0.003 – 0.006. In this paper and in Paper II we did take into account temperature variations and therefore there is no systematic difference due to this effect between our two Y_p determinations. On the other hand, when comparing our results with those of other authors who assume a constant temperature given by $T(4363/5007)$, a systematic difference is present that has to be taken into account.

From the analysis of the data studied in this paper we derive a Y_p value of 0.2477 ± 0.0029 for $t^2 \neq 0.000$, while under the assumption of $t^2 = 0.000$, we obtain that $Y_p = 0.2523 \pm 0.0027$. From the Y_p given by the WMAP results combined with the adoption of the SBBN, if our error budget is correct, our result implies that t^2 has to be larger than zero at more than the 1- σ level.

It has been argued that the uncertainty on Y_p is dominated by systematic errors (Olive & Skillman 2004). If this is the case, it is certainly preferable to analyze a few objects in depth and try to correct for the systematic errors, than to rely on a statistical analysis of a large sample, since this last method can reduce the statistical errors but not the systematic ones.

From Table 8 it follows that the Y_p , D_p , and *WMAP* observations are in very good agreement with the SBBN predicted values. Moreover our Y_p value, if our error budget is correct, provides stronger constraints to some predictions of non-standard Big Bang cosmologies than previous studies (e.g. Cyburt et al. 2005; Coc et al. 2006, and references therein).

The authors wish to thank Miguel Cerviño for help with the high resolution synthesis models and Gary Ferland for several discussions on this topic. We are grateful to the referee for the detailed reading of the manuscript and many excellent comments and suggestions. We also acknowledge fruitful correspondence with R. L. Porter, K. B. MacAdam, and G. Steigman. The high-resolution synthesis models used in this work have been retrieved from PGos3 (<http://ov.inaoep.mx/pgos3>), which is operated by the future Mexican Virtual Observatory. This work was partly supported by the CONACyT grant 46904 and by the Spanish *Programa Nacional de Astronomía y Astrofísica* through projects AYA2004-02703 and AYA2004-07466. VL acknowledges the hospitality of IA-UNAM and INAOE, where a part of this research was carried out, and the support of a *CSIC-I3P* fellowship.

REFERENCES

- Aller, L. H. 1984, *Physics of Thermal Gaseous Nebulae* (Dordrecht: Reidel)
- Anderson, H., Ballance, C. P., Badnell, N. R., & Summers, H. P. 2000, *Journal of Physics B Atomic Molecular Physics*, 33, 1255
- Anderson, H., Ballance, C. P., Badnell, N. R., & Summers, H. P. 2002, *Journal of Physics B Atomic Molecular Physics*, 35, 1613
- Bauman, R. P., Porter, R. L., Ferland, G. J., & MacAdam, K. B. 2005, *ApJ*, 628, 541
- Benjamin, R. A., Skillman, E. D., & Smits, D. P. 1999, *ApJ*, 514, 307
- Benjamin, R. A., Skillman, E. D., & Smits, D. P. 2002, *ApJ*, 569, 288
- Blagrave, K. P. M., Martin, P. G., Rubin, R. H., Dufour, R. J., Baldwin, J. A., Hester, J. J., & Walter, D. K. 2007, *ApJ*, 655, 299

- Brocklehurst, M. 1971, MNRAS, 153, 471
- Callaway, J. 1994, Atomic Data and Nuclear Data Tables, 57, 9
- Cardelli, J. A., Clayton, G. C., & Mathis, J. S. 1989, ApJ, 345, 245
- Coc, A., Nunes, N. J., Olive, K. A., Usan, J.-P., & Vangion, E. 2006, astro-ph/0610733
- Code, A. D. 1960, in Stellar Atmospheres, Vol. VI of Stars and Stellar Systems, ed. J. L. Greenstein (Chicago: University of Chicago Press), p. 50
- Cyburt, R. H., Fields, B. D., Olive, K. A., & Skillman, E. 2005, Astroparticle Physics, 23, 313
- Davidson, K., & Kinman, T. D. 1985, ApJS, 58, 321
- Ferland, G. J. Korista, K.T. Verner, D.A. Ferguson, J.W. Kingdon, J.B. Verner, & E.M. 1998, PASP, 110, 761
- Fukugita, M., & Kawasaki, M. 2006, ApJ, 646, 691
- González Delgado, R. M., Cerviño, M., Martins, L. P., Leitherer, C., & Hauschildt, P. H. 2005, MNRAS, 357, 945
- González Delgado, R. M., Leitherer, C., & Heckman, T. M. 1999, ApJS, 125, 489
- Izotov, Y. I., Chaffee, F. H., Foltz, C. B., Green, R. F., Guseva, N. G., & Thuan, T. X. 1999, ApJ, 527, 757
- Izotov, Y. I., Schaerer, D., Blecha, A., Royer, F., Guseva, N. G., & North, P. 2006, A&A, 459, 71
- Izotov, V. I., & Thuan, T. X. 2004, ApJ, 602, 200
- Izotov, Y. I., Thuan, T. X., & Lipovetsky, V. A. 1997, ApJS, 108, 1
- Kingdon, J., & Ferland, G. 1995, ApJ, 442, 714
- Leone, F., & Lanzafame, A. C. 1998, A&A, 330, 306
- Luridiana, V. 2003, proceedings of the XXXVIIth Moriond Astrophysics Meeting “The Cosmological Model” eds. Y. Giraud-Héraud, C. Magneville, J. Tran Thanh Van, The Gioi Publishers (Vietnam), 159 (astro-ph/0209177)
- Luridiana, V., Peimbert, A., Peimbert, M., & Cerviño, M. 2003, ApJ, 592, 846 (Paper II)

- Luridiana, V., Peimbert, M., & Leitherer, C. 1999, ApJ, 527, 110
- Miller, J. S. & Mathews, W. G. 1972 ApJ, 172, 593
- O’Dell, C. R., & Hubbard, W. B. 1965, ApJ, 142, 591
- O’Dell, C. R., Hubbard, W. B., & Peimbert, M. 1966, ApJ, 143, 743
- Olive, K. A., & Skillman, E. D. 2004, ApJ, 617, 29
- O’Meara, J. M., Burles, S., Prochaska, J. X., Prochter, G. E., Bernstein, R. A., & Burgess, K. M. 2006, ApJ, 649, L61
- Osterbrock, D. E., & Ferland, G. 2006, *Astrophysics of Gaseous Nebulae and Active Galactic Nuclei* (Mill Valley: University Science Books)
- Osterbrock, D. E., & Flather, E. 1959, ApJ, 129, 26
- Peimbert, A. 2003, ApJ, 584, 735
- Peimbert, A., Peimbert, M., & Luridiana, V. 2002 ApJ, 565, 668 (Paper I)
- Peimbert, M. 1966, ApJ, 145, 75
- Peimbert, M. 1967, ApJ, 150, 825
- Peimbert, M., Peimbert, A., Luridiana, V. & Carigi, L. 2007, in *From Stars to Galaxies: Building the Pieces to Build up the Universe*, eds. A. Vallenari, R. Tantaló, L. Portinari, & A. Moretti, ASP Conference Series, in press, astro-ph/0701313, 2007.
- Peimbert, M., Peimbert, A., Luridiana, V. & Ruiz, M. T. 2003, in *Star Formation through Time*, ASP Conference Series 297, 81, (astro-ph/0211497)
- Peimbert, M., Peimbert, A., & Ruiz, M. T. 2000, ApJ, 541, 688
- Peimbert, M., & Torres-Peimbert, S., 1974, ApJ, 193, 327
- Porter, R. L., Bauman, R. P., Ferland, G. J. , & MacAdam, K. B. 2005, ApJ, 622L, 73
- Porter, R. L., Ferland, G. J., & MacAdam, K. B. 2007, ApJ, 657, 327
- Relaño, M., Peimbert, M., & Beckman, J. 2002, ApJ, 564, 704
- Robbins, R. R., & Bernat, A. P., 1973, Mem. Soc. R. Sci. Liege, 5, 263
- Robbins, R. R., & Bernat, A. P., 1974, ApJ, 188, 309

- Sawey, P. M. J., & Berrington, K. A., 1993, *Atomic Data and Nuclear Data Tables*, 55, 81
- Skillman, E. D., Terlevich, E., & Terlevich, R., 1998 *Space Sci. Rev.*, 84, 105
- Smits, D. P. 1996, *MNRAS*, 278, 683
- Spergel, D. N. et al. 2006, *astro-ph/0603449*
- Stasińska, G., & Izotov, Y. I. 2001, *A&A*, 378, 817
- Steigman, G. 2006a, *Int. J. Mod. Phys. E*, 15, 1, *astro-ph/0511534*
- Steigman, G. 2006b, *astro-ph/0606206*
- Storey, P. J., & Hummer, D. G. 1995, *MNRAS*, 272, 41
- Vriens, L., & Smeets, A. H. M. 1980, *Phys. Rev. A*, 22, 940
- Whitford, A. E. , 1958, *AJ*, 63, 201